Optimal Tuning of Fractional Order Controllers for Rotational Speed Control of UAV's Propulsion Unit Based on an Iterative Batch Method

Wojciech Giernacki*, Dariusz Horla*, Talar Sadalla*, Tadeo Espinoza Fraire**

**Faculty of Electrical Engineering, Institute of Control, Robotics and Information Engineering, Poznan University of Technology, ul. Piotrowo 3A, 60-965 Poznań, Poland (e-mail: wojciech.giernacki@put.poznan.pl)*
***Faculty of Engineering, Science and Architecture, Univesidad Juárez del Estado de Durango, Av. Universidad S/N, Fracc. Filadelfia, C.P. 35070, Gómez Palacio, Durango, México*

Abstract: The paper presents an optimal batch method for tuning easy-to-implement controllers with fixed parameters, which are widely used to control propulsion units in unmanned aerial vehicles (UAVs) in rotational speed control task of the propellers. As a result of the latter, this method might be used to satisfy thrust demand defined by profile of a reference thrust force. In the proposed approach, tuning of a fractional-order proportional-integral controller (FOPI) is performed on the basis of a linear model of the propulsion unit. By using Hermite-Biehler and Pontryagin theorem, the range of controller parameters ensuring stability of the closed-loop system (rotational speed control) is obtained. In this range, or within the area of fail-safe parameters, the optimal choice of gains of a FOPI controller is performed, on the basis of the predefined cost function minimized off-line by a zero-order algorithm. In the paper, sample simulation results are presented, which have been obtained for the model of the propulsion unit used in multirotor UAVs. These results refer to data obtained in prior with a proportional-derivative-integral (PID) controller, CDM controller tuned by Coefficient Diagram Method, near-to-optimal fractional-order PID controller tuned by Best-from-the-best procedure and FOPI controller tuned by SCoMR-FOPI procedure.

Keywords: UAV, fractional-order controller, propulsion unit, Hermite-Biehler and Pontryagin theorems, Fibonacci algorithm, optimal tuning, optimization.

1. INTRODUCTION

Factors such as dynamics, expected performance and maximum duration of flight of unmanned aerial vehicles depend on the choice of propulsion units to a great extent (Won Kim and Brown, 2010; Bondyra et al., 2016; Aleksandrov and Penkov, 2012). During implementations of solutions in particular constructions, starting from the class of Micro Aerial Vehicles (MAVs), both multirotor and fixed-wing vehicles, unpaired, single, propulsion units are still commonly used. Every unit is composed of the motor, which is usually a brushless DC motor, a propeller mounted directly on the shaft of the motor and an Electronic Speed Controller (ESC) – see Fig. 1. This module is responsible for driving the DC motor via sufficiently fast changes in Pulse Width Modulation (PWM) duty cycles, leading to the generated thrust and torque. The majority of available solutions, especially in model scale, on the contrary to the name of ESC, does not have any possibility to control, or even to measure, the effective rotational speed of the propellers or of a generated thrust force, thus there is no feedback from those signals from the output of propulsion unit. Such an architecture results in many drawbacks, especially severe and visible in multirotor MAVs, where fast dynamics of the propulsion units and low mass of the construction of a UAV combined with no possibility to control rotational speed of consecutive units, leads often to misbalanced thrust forces. Declared, reference values of rotational speeds differ from real ones due to multiple reasons, disturbances, mechanical wear of the propulsion units of low battery state in UAVs. As the result, current position and orientation of a MAV is different from the declared one, what is one of the most elementary and still valid problems faced by control theory and robotics (Raptis and Valavanis, 2011; Valavanis and Vachtsevanos, 2015; Guo, 2015). In the last years, an increased number of practical applications stipulated increase in scientific interest in which stabilization and improvement of flying-characteristics capabilities is expected.

Fig. 1. Components of the propulsion unit and their mounting place in an unmanned aerial vehicle.

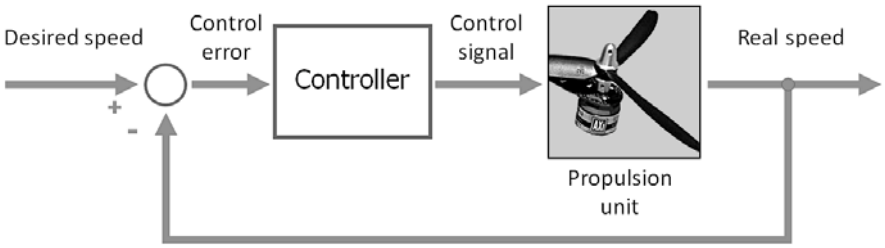

Fig. 2. Rotational speed closed-loop control system.

These applications include amongst the other: video recording from a stabilized or slowly-moving flying platform, autonomous landing, grasping objects in flight, transportation tasks (Pounds et al., 2012) or virtual missions of multi-robot systems (Zelazo et al., 2015; Saska et al., 2016).

Possible tasks to stabilization of position and orientation of MAVs are sought in higher control layers then rotational speed control, i.e. in direct control loops of orientation and position of UAVs, by controlling thrust forces and angular torques. Further information can be found in classical references, as (Mahony et al., 2012; Castillo et al., 2005; Ren et al., 2012), and a spectrum of the proposed control algorithms is wide (from simple, fixed-parameter controllers of PID type (Bouabdallah et al., 2004), self-tuning nonlinear controllers (Gautam and Ha, 2013), event-based control (Durand et al., 2018), ending on using bio-inspired techniques, see (Fister et al., 2016, Duan and Li, 2014)). In the context of angle stabilization in fixed-wing UAV when using linear and nonlinear controllers, the comparison of their performance can be found, e.g., in (Espinoza et al., 2013; Espinoza et al., 2018).

2. PROBLEM STATEMENT

The main point of this paper is to focus on the lowest layer of a control system, i.e. rotational speed control of a single propulsion unit (Fig. 2), as in (Magsimo et al., 2013; Sanchez et al., 2011), assuming that linear models are used, as in (Gardecki et al., 2013), and, on the contrary to the approaches proposed in (Szafrański et al., 2014; Gąsior et al., 2016), aiming at the use of more sophisticated control techniques as proposed therein. The authors are interested in using a simple PI controller which performance can be enhanced by generalization of its mathematical description with the use of fractional-order operators.

By introduction of a fractional-order of integration λ to a controller, a visible improvement in the shaping of frequency response of a control system can become visible, as no longer the slope of an integer multiplicity of 20dB can be attained. More benefit from the application of fractional-order controllers (especially for practicing engineers using full flexibility offered by fractional-order mathematics) can be found in (Efe M. Ö., 2011).

In (Giernacki et al., 2017a), Hermite-Biehler and Pontryagin theorems have been used to obtain a stability region estimate in which controller parameters in a continuous-time FOPI structure are sought, in accordance with the proposed procedure for modelling and rotational Speed Control of Motor-Rotor unit (SCoMR-FOPI procedure). In the paper, a mechanism of optimal tuning of controller parameters is implemented, what is the added value to the approach. The basic aim of the mechanism is to ensure rapid tuning and perform fairly simple calculations, what is of prime importance taking the lowest-level control layer requirements (rotational speed control in UAVs) into account.

From the variety of optimization techniques (see eg. Precup et al., 2015, Chong and Zak, 2001, Killingsworth and Krstic, 2006, Duan and Li, 2014), the one used in this paper is based on the Fibonacci-search method and bootstrapping technique. It has primarily been developed for off-line, model-based optimal auto tuning of the fixed-wing UAV orientation controllers (PD type) (Giernacki et al., 2018b) and for real-time model-free optimal auto tuning of the multirotor UAV altitude controller (PD type) (Giernacki et al., 2018a). Both cited references confirmed the applicability of the method and its low computational complexity when tuning controllers of upper (an one order slower) UAV control layers. In the both cited references, the proposed tuning methods have not guaranteed, however, stability of the control system, what is the main characteristics of the proposed approach. The latter comes as a result of using the analytical model of the propulsion unit and stability condititons derived for a fractional-order system.

The main contributions of this paper are the following:

- presentation of a novel approach to zero-order, off-line optimal gain tuning of rotational speed controllers used in unmanned aerial vehicles based on optimization algorithm via bootstrapping technique and Fibonacci-search method,

- outline of a simple prototyping synthesis method, of the control system of the rotational speed with continuous-time fractional-order controller in a FOPI structure. The controller parameters are optimal and chosen from a box in a stability area of the closed-loop system obtained by the use of Hermite-Biehler and Pontryagin theorems,

- giving a study of performance of the proposed optimization strategy for integer-order (PI) and fractional-order (FOPI) type controllers by specific, comparative simulation tests for the dynamical model of the driving unit (used in the Hornet quadrotor – Fig. 3), obtained on the basis of experiments conducted on a special laboratory test stand – Fig. 4 (Gardecki et al., 2013). The expectations towards a rapid and overshoot-free tracking of rotational speed have been expressed by a proper choice of a minimized aim function based on the error signal samples.

Fig. 3. The Hornet quadrotor developed at the Institute of Control, Robotics and Information Engineering of Poznan University of Technology (*propulsion units used in experiments).*

The paper is organized as follows: Section III presents the steps of the proposed procedure of optimal tuning of FOPI controllers in rotational speed tracking problem in UAVs. Sections IV-VI give a deeper insight into the procedure, and, respectively, Section IV includes the description of a synthesis of the rotational speed control system with a FOPI controller, Section V discusses stability issues, and Section VI presents the optimal tuning method. Comparative tests performed by means of simulations have been included in Section VII, and Section VIII presents conclusion.

3. PROCEDURE FOR OBTAINING OPTIMAL PARAMETERS OF A FOPI CONTROLLER

The problem of optimal tuning of a fractional-order controller with N parameters within the predefined ranges on the basis of a minimization task of the function $J(t)$ can be ingeneral expressed as:

$$\min_{K_1,K_2,\ldots,K_N} J(t)=\int_0^{t_h}|e(\tau)|d\tau \quad \text{subject to}: \begin{array}{l} 0\le K_1\le K_1^{\max} \\ 0\le K_2\le K_2^{\max} \\ \ldots \\ 0\le K_N\le K_N^{\max} \end{array} \tag{1}$$

In the example, considered in the remaining part of the paper, there is a pair of gains sought in a time horizon t_h of a fractional-order controller (K_P and K_I) with the proposed procedure. The cost function values are based on Integral of Absolute Error – IAE measure, obtained on the basis of measurements of the tracking error $e(t)$. The proposed method requires one to perform n identical simulation, by comparing n IAE values for n various controller gains pairs. By using the Fibonacci-search algorithm to search for optimal controller gains and bootstrapping technique to switch between tuned parameters, shortens the exploration time among all possible pairs of gains, by stipulating only those for which IAE is decreasing, and the use of Hermite-Biehler and Pontryagin Theorems with two BIBO (Bound-Input Bounded-Output) conditions allows one to contract the ranges for controller gains only to those, where the stability of the closed-loop system is ensured. This is also important from the following reason: a proper choice of $J(t)$ can mirror the expectations towards transients in a closed-loop system.

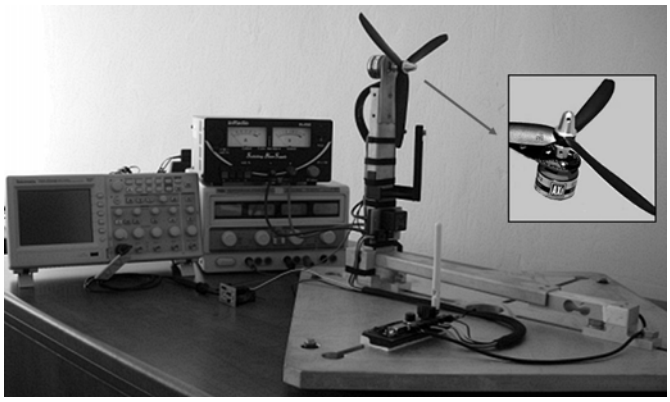

Fig. 4. Propulsion unit used in the experiments on test stand.

In the example, the proiority choice was to ensure fast and and overshoot-free speed changes in a UAV, thus the function $J(t)$ is absolute tracking error value-based.

The proposed procedure is composed of the following steps, described in detail in the further part of the text:

1. Obtain a model of the plant, i.e. of the motor unit of the UAV, in a form of a transfer function $G(s)$ – see (1) from Section 4.1.

2. Stipulate a priori values of λ (fractional order operator in the integral term) for which optimal parameters of FOPI controllers will be found. For a more detailed information about the FOPI controller and reasonable values of the λ parameter, see Section 4.2.

3. Use Hermite-Biehler and Pontryagin Theorems and two BIBO conditions (explained in Section 5) to obtain a stability region estimates for each of FOPI controllers.

4. Search for optimal continuous-time controller parameters by the use of the Fibonacci-search algorithm and bootstrapping technique.

5. Verify performance of tracking of rotational speed in closed-loop systems with the FOPI controllers obtained from Step 4.

6. Choose the controller with the preferred dynamics.

7. (Optional) Transform the obtained continuous-time model of the controller with the use of Oustaloup approximation into its sampled-data version, which is easy to implement in embedded systems of a multirotor control architecture of UAVs. This step is not considered in the paper due to a limited space. An in-depth information concerning how to obtain discrete-time controller models using Oustaloup approximation can be found, e.g., in (Tepljakov, 2017).

4. A ROTATIONAL SPEED CONTROL SYSTEM FOR A LINEAR MODEL OF THE PROPULSION UNIT AND A FOPI CONTROLLER

The control task with rotational speed as output signal, is performed in a standard negative feedback system, where the continuous-time linear model of the propulsion unit is described by a transfer function. In a similar way, a FOPI controller is described, however, in its case, a fractional order (λ) operator in the integral term ($1/s^{\lambda}$) is used.

4.1 Mathematical model of propulsion unit

An in-depth description of the process of acquiring data and methods to identify models can be found in (Gardecki et al., 2013; Giernacki et al., 2017a,b; Giernacki, 2016a), which are applied in order to derive a linear mathematical model of the driving unit. In the current paper, only the equation defining the model is cited, presented in a form of a first-order inertia model with transport delay (L). It is presented as

$$G(s)=\frac{\Omega(s)}{V(s)}=\frac{b_0}{a_1 s+a_0}e^{-sL}=\frac{1}{0.04\,s+1}e^{-0.35\,s}, \tag{2}$$

what forms a starting point for further synthesis, where $\Omega(s)$ and $V(s)$ are Laplace transforms of the rotor rotational speed $\omega(t)$ and the input signal $v(t)$ applied to the electronic speed controller.

Model (2) is presented with full reference to the dynamics of *AXI 2814/12 GOLD LINE BLDC* motor – *Model Motors* combined with *GWS-HD9050x3-SW 9x5″* (three-bladed propeller) and with *T18A (T-Motors)* 3-phase AC ESC (see Fig. 1). This propulsion unit achieves its maximum thrust at the level of 19.09 N with PWM=77 %, RPM=8893 r/min. The maximum speed RPM=9039 r/min is obtained at PWM=75 % and useful thrust ranges from 3.924 N (RPM=4492.5 r/min). The rotational speed corresponding to the gain of 1 in below models is equal to the value of 9550.25 r/min.

4.2 FOPI controller basics

Introducing an additional controller parameter λ denoting a fractional-order of integration, an increase in accuracy of design in closed-loop system's frequency characteristics might be achieved. Now, the slope is not constrained only to multiplicity of *20log(gain)*, but also to its fractional multiplications. For previous research results on fractional-order see e.g. (Giernacki et al., 2017a; Giernacki, 2016a).

The authors of (Chen et al., 2009) state that fractional calculus generalizes differentiation and integration to fractional order fundamental (continuous integro-differential) operator ${}_aD_t^r$:

$${}_aD_t^r=\begin{cases}\dfrac{d^r}{dt^r} & r>0\\ 1 & r=0.\\ \displaystyle\int_a^t (d\tau)^{-r} & r<0\end{cases} \tag{3}$$

In (3) a and t are the operation limits; r – operation order, which is generally a real value.

Below, the Riemann-Liouville definition of the fractional differo-integral is used:

$${}_aD_t^r(t)=\frac{1}{\Gamma(n-r)}\left(\frac{d}{dt}\right)^n\int_a^t\frac{f(\tau)}{(t-\tau)^{1-n+\alpha}}d\tau, \tag{4}$$

where $n-1<r<n$, and $\Gamma(\cdot)$ is the Euler's Gamma function. As in integer-order systems, the Laplace transform of (4), can be used, which is defined as:

$$\int_0^\infty e^{-st}\,{}_0D_t^r f(t)dt=s^r F(s)-\sum_{k=0}^{n-1}s^k\,{}_0D_t^{r-k-1}f(t)\Big|_{t=0} \tag{5}$$

for $n-1<r<n$.

In Eqn. 5, s operator denotes the Laplace transform variable and $s=j\omega$.

Furthermore, from Eqn. 5, it is therefore possible to set the structure of FOPI (denoted as PI$^\lambda$) controller type to following form:

$$C(s)=K_P+K_I s^{-\lambda}. \tag{6}$$

In Eqn. 6, the variable K_P means the proportional gain, variable K_I means integration gain and λ – positive real number.

Note: In the most often case, for the synthesis of closed-loop control system with fractional-order controllers, the λ value is set between 0 and 1.

5. USE OF HERMITE–BIEHLER AND PONTRYAGIN THEOREMS

The closed-loop characteristic quasi-polynomial $\delta(s)$ referring the system with the controller $C(s)$ from (6) is given by:

$$\delta(s)=\left(b_0K_P+b_0K_I s^{-\lambda}\right)e^{-sL}+a_1 s+a_0. \tag{7}$$

When the value of λ is fixed, a stabilizing range for the K_P and K_I parameters can be obtained on the basis of Hermite-Biehler and Pontryagin theorems (see Appendix A and B). The latter can be done when all roots of (7) are real and interlaced, and when it is possible to estimate the stabilizing ranges using a pair of BIBO stability conditions (details at the end of the section). Then, zero-order iterative method combined with bootstrapping technique is proposed to find optimal values of K_P and K_I parameters in predefined ranges.

Considering δ from the Eqn. 7 as a complex function of ω, the following equation can be formulate:

$$\delta^*(j\omega)=\delta_r^*(\omega)+j\delta_i^*(\omega). \tag{8}$$

In Eqn. 8, $\delta_r^*(\omega)$ and $\delta_i^*(\omega)$ are the real and imaginary parts of $\delta^*(j\omega)$ and in accordance with Pontryagin Theorem, $\delta_r^*(\omega)=0$ and $\delta_i^*(\omega)=0$.

Based on the above equations, and according to Appendix C (equations C4-C5), the parameter K_P can be described by the following formula:

$$\begin{aligned}K_P=&\left[-\frac{a_0}{b_0}\cos(\omega)+\frac{a_1\omega}{b_0L}\sin(\omega)\right]+\\ &-\left[\frac{a_1\omega}{b_0L}\cos(\omega)+\frac{a_0}{b_0}\sin(\omega)\right]\frac{\left|\mathrm{Re}(j)^{a/b}\right|}{\left|\mathrm{Im}(j)^{a/b}\right|}sign(\omega).\end{aligned} \tag{9}$$

As in (Bellman and Corke, 1963), the stabilizing range for K_I should satisfy:

$$\begin{aligned}&\max_\omega\left(-m_j(\omega)K_P-b_j(\omega)\right)<K_I,\\ &K_I<\min_\omega\left(-m_j(\omega)K_P-b_j(\omega)\right)\quad j=0,1,2,...\end{aligned} \tag{10}$$

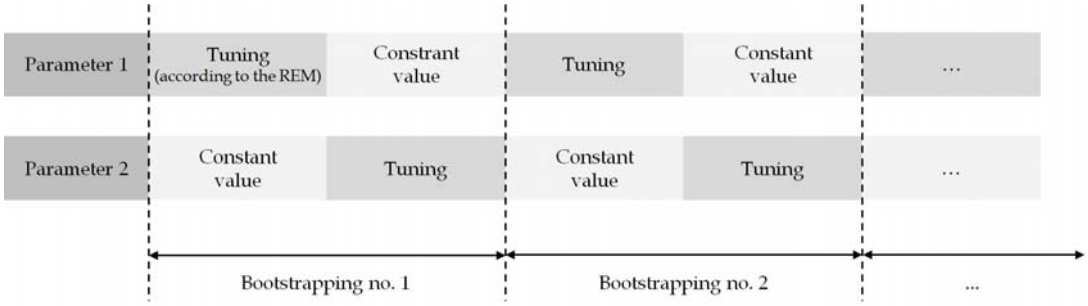

Fig. 5. Idea of the bootstrapping mechanism.

where

$$m(\omega) = -\left|\mathrm{Re}(j)^{a/b}\right| \frac{\left|\omega^{a/b}\right|}{L^{a/b}}, \tag{11}$$

and

$$b(\omega) = \left[-a_0 \cos(\omega) + \frac{a_1\omega}{L}\sin(\omega)\right]\left|\mathrm{Re}(j)^{a/b}\right| \frac{\left|\omega^{a/b}\right|}{L^{a/b}} + \\ -\left[a_0 \sin(\omega) + \frac{a_1\omega}{L}\cos(\omega)\right]\left|\mathrm{Im}(j)^{a/b}\right| \frac{\left|\omega^{a/b}\right|}{L^{a/b}} sign(\omega) \tag{12}$$

result from rewritten polynomial $\delta_r^*(\omega)$ to the form:

$$\delta_r^*(\omega) = b_0 K_I - m(\omega) K_P - b(\omega). \tag{13}$$

Since $\delta_i^*(\omega)$ is an odd function, it has the root at ω=0. Thus, for $\omega=\omega_0$=0:

$$\delta_i^*(\omega) = b_0 K_P + a_0. \tag{14}$$

To ensure the interlace property between real $\delta_r^*(\omega)$ and imaginary $\delta_i^*(\omega)$ part of (8), the following condition results:

$$\delta_i^*(\omega) > 0 \Rightarrow b_0 K_P + a_0 > 0 \Rightarrow K_P > -a_0 / b_0. \tag{15}$$

The rotational speed control system is considered stable, if a pair of BIBO-like criteria is met:

- when the simulation time corresponds to the defined horizon of simulation (they needs to be the same),

- when the closed-loop output signal system does not diverge, either exponentially of in the oscillatory manner.

If any of the two conditions is not met, the closed-loop system is considered to be unstable.

6. FIBONACCI–SEARCH METHOD

When the model of a plant is not available, or cannot be presented in analytical form, or the form of the cost function implies that gradient/Hessian information cannot be used, making additional assumptions can lead to using the considered optimization approach. Among such assumptions one can identify the unimodal cost function.

At every optimization stage, one optimal point is sought, and using branch-and-bound strategy, the range embracing the optimum point is reduced. Also the cost function is calculated, as e.g. sum of squared tracking error samples over a horizon for repeated reference trajectory primitive. Following that, the optimization function accepts its value to reduce the range.

Suppose that for the sample range [0, 1] of parameter x, a pair of values of the function is obtained, namely $f(x^{(k-)})$ and $f(x^{(k+)})$ for two candidate points ('-' symbol refers to left candidate point, interior point of the range [0, 1], and '+' – to the right candidate point):

$$\begin{aligned} x^{(k^-)} &= x^{(k-1^-)} + \rho_k \left(x^{(k-1^+)} - x^{(k-1^-)}\right) \\ x^{(k^+)} &= x^{(k-1^-)} + (1-\rho_k)\left(x^{(k-1^+)} - x^{(k-1^-)}\right), \end{aligned} \tag{16}$$

where $\rho_k = F_{N-k}/F_{N-k+2}$ denotes the reduction ratio of the initial range between iterations, calculated as the ratio of the Fibonacci numbers (see (Chong and Zak, 2001) for further details).

For the specific feature of the cost function, the range where optimum is sought can be reduced whenever it is ensured that it remains inside it. The algorithm terminates, when after N iterations the range decreases below a relative length if the initial one.

This approach can be used in bootstrap sequences in a two-parameter optimization, assuming that one of the parameters is kept constant and the other is found on the basis of this iterative procedure, and, secondly, the first one is kept constant (calculated on the basis of the prior iterations), and the other is tuned (Fig. 5). This forms a single bootstrap that is run in a loop.

This can be put in the following pseudocode:

1. Assume safe ranges of parameters R_1 and R_2 for a two-parameter controller, initial value of the second parameter and stipulate stopping condition (accuracy) with the number of bootstraps,

2. Assume the second parameter is constant (taken as the result of the previous iteration or as initial value), and perform Fibonacci search for the first parameter in the range R_1,

3. Assume the first parameter is constant (taken as the result of the previous step), and perform Fibonacci search for the second parameter in the range R_2,

4. If the number of bootstraps is not exceeded, proceed to step 2), otherwise stop the algorithm.

If the cost function is not unimodal, the method should be used for various initial ranges, to identify multiple minima, to identify the global one.

7. COMPARATIVE TESTS

A series of simulation tests has been performed using MATLAB/Simulink environment, to evaluate the proposed optimal tuning method of a fixed-gain controller in a FOPI structure in a closed-loop system with the model of the propeller unit (see Section IV) taking step disturbances into account (mirroring effects of wind gusts acting on the blades of propellers), and with control amplitude constraints (here, u_{max}=±6). Controllers have been tuned in a tracking problem of rectangular reference signal with amplitude equal to 1, the period equal to 0.8 sec in 2 second simulation horizon. It has been expected, to obtain a rotational speed control in UAV at the greatest possible pace and with no overshooots.

This paper presents results and analysis of four numerical tests, with the range of parameters K_P and K_I calculated by using equation (9) and inequalities (10) and (15). Furthermore, there has been a supplementary material added to the Mathematical Models Database (http://mathematicalmodels.put.poznan.pl) in a form of source codes (MATLAB m.files) and Simulink block diagrams used in the current paper, to infer conclusions of comparatory tests from efficiency of different controller types. In the case of fractional-order controllers their implementation has been carried out with the use of a FOMCON toolbox (http://fomcon.net) – for details please refer to (Tepljakov et al., 2017). The model of a continuous-time fractional-order controller has been subject to the Oustaloup-Recursive-Approximation used in FOMCON toolbox for Fractional Order integrator in the Matlab environment. The approximation parameters of fractional-order integrator the order was equal to 5 and frequency range was (0.001, 1000) rad/sec sampling period for continuous-time approximation of fractional-order integration was 0.01 sec. The examples below present the methodology of obtaining controller parameters, with the most important configuration parameters for the fractional-order and other controllers presented in Table no. 1. The detailed synthesis description can be found in the prior work of the authors, cited in the caption to Figure 8.

An in-depth analysis has been conducted with special attention paid to effectiveness of the optimization of parameters of a FOPI controller (K_P and K_I) for fixed values of λ (in the tests, it has been assumed that these parameters fall in the range from 0.1 to 1.0 with an increment of 0.1, i.e. for controllers $PI^{0.1}$-$PI^{1.0}$). A two-dimensional parameter search space grid, with values of cost functions, i.e. integral performance indexes of I_1 (IAE) have been returned for, has been obtained for every λ on the basis of Hermite-Biehler and Pontryagin theorems.

The obtained ranges of parameters ensuring stability have finally been reduced to the range presented in Figure 6, in order to be able obtain them in an iterative manner, with surface I_1=f(K_P, K_I) drawn, e.g. see the case of the controller $PI^{0.1}$ presented in Figure 6. By doing so it became possible to verify if the Fibonacci-search method combined with bootstrapping technique actually finds the global minimum of

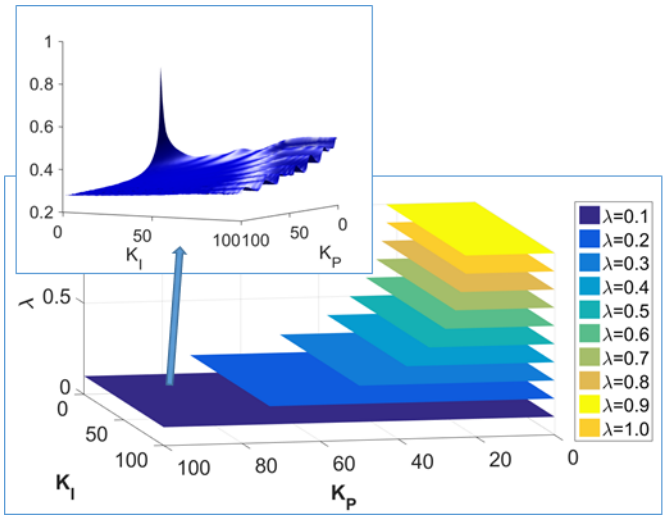

Fig. 6. Stability regions *obtained* from *Hermite-Biehler and Pontryagin theorems (*saturated to: K_{Pmax}=*100,* K_{Imax}=*100)* of parameters K_P, K_I *for change of* λ values from 0.1 to 1 for closed-loop control system with plant model (2): ω value from -200 to 200 (step: 4 rad/s); above: sample I_1=*f*(K_P, K_I) *function for* $PI^{0.1}$ *controller*.

Table 1. Parameters of controllers used in comparatory tests accompanied by basic performance indices.

	CDM	*PID tuner*	*PID SROT*	FOPID	*SCoRM -FOPI*	FOPI optimal
K_P	-	21.3	3.24	3.24	21.86	91.7
K_I	-	267	49.4	49.4	14.41	7.01
K_D	-	0.426	0.06	0.06	-	-
λ	-	-	-	0.02	0.01	0.01
μ	-	-	-	1.33	-	-
Other sets	A(s)= $0.0008s^2$+0.36s B(s)=$0.0001s^2$+ 0.0196s+1 F(s)=1	-	-	-	-	-
IAE	0.1611	0.4445	0.4670	0.2646	0.3126	0.2843
ISE	0.0780	0.3859	0.4097	0.3275	0.3349	0.3351

I_1 with given accuracy. In the paper (Giernacki et al., 2017a), the parameters K_P and K_I (marked with triangles, see Fig. 7a) have been obtained with accuracy 10^{-2}. The method proposed in this paper allowed to increase this accuracy to up to 10^{-4}.

In order to do so, two series of tests have been conducted, with initial values for K_P and K_I parameters equal to 10 assumed in both tests, performing consecutive bootstraps, seeking in an iterative manner for parameters K_P and K_I minimizing by Fibonacci-search method of I_1 for the following cases:

- Test 1: stopping criterion = 0.005, accuracy of Fibonacci-search method = 0.001, delta parameter for the last Fibonacci-search iteration (i.e. to perform dichotomy-like iteration) = 0.01, limit of main iterations = 20,

- Test 2: respectively: 0.0001, 0.0001, 0.001, 100.

The results have been presented in Table 2 and Figure 7, where graphical results of convergence of the algorithm have also been included for several pairs of initial K_P and K_I (Test III). Figure 8 presents the comparison of tracking

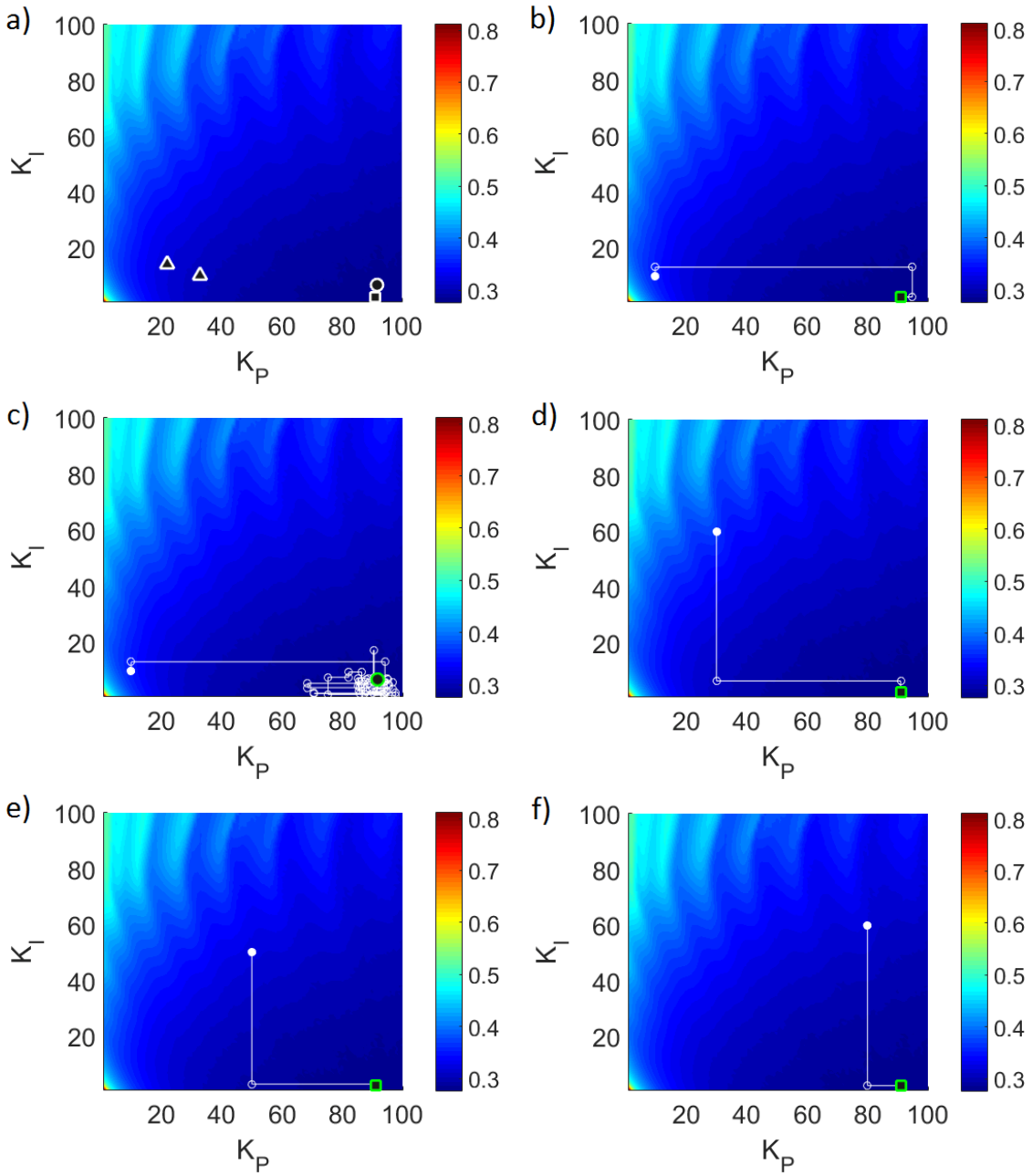

Fig. 7. Surface $I_1=f(K_P, K_I)$: a) local minima obtained from SCoMR-FOPI method (Giernacki et al., 2017) (triangles – controllers $PI^{0.1}$ and $PI^{0.49}$), controller $PI^{0.1}$ from Test I (squares), controller $PI^{0.1}$ from Test II (circles), b)-c) convergence of the proposed algorithm for $PI^{0.1}$ controller (Test I and II), d)-f) convergence of the proposed algorithm for $PI^{0.1}$ (Test no. III).

performance for the optimal FOPI controller with controllers presented in following papers (Gardecki et al., 2013; Giernacki et al., 2017a; Giernacki, 2016a) – Test IV. The comments to the results of simulations tests have been included in Conclusion Section.

8. CONCLUSION

In the paper, the optimal tuning method of FOPI controllers in an rotational speed tracking problem has been presented in the system with a model of the sample driving unit used in UAVs. The efficiency of the proposed method has been verified on the basis of four tests.

The major conclusions include:

- The proposed method allows to limit the search space of optimal controller parameters to the range, in which the prototyped closed-loop system is stable. In the simulation tests it has turned out to be sufficient to have grid of 10^6x10^6 points in the case of a $PI^{0.1}$ controller, for which the lowest value of I_1 has been obtained, with the improvement of 6.6 % with reference to I_1 for $PI^{0.49}$ with SCoRM-FOPI method (Giernacki et al., 2017a),

- By decreasing λ, a decrease in I_1 can be observed, with increase in K_P and decrease of K_I,

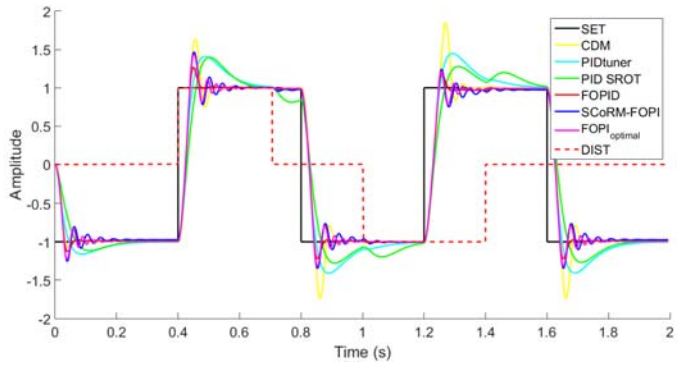

Fig. 8. Reference signal (SET) tracking in disturbed (DIST) systems with Coefficient Diagram Method (CDM) controller *(Gardecki et al., 2013)*, two PID controllers tuned by MATLAB PID Tuner and Simulink Optimization Toolbox (SROT) *(Giernacki, 2016a)*, as well as FOPID and FOPI controllers tuned by Best from the best *(Giernacki, 2016a)*, SCoMR-FOPI *(Giernacki et al., 2017a)* and Fibonacci-search method *(Giernacki, 2018b)*, respectively.

- By increasing the accuracy of the algorithm (see Test III), the number of main iterations increases, as well the number of required bootstraps (see Fig. 7e) in order to achieve even a slight improvement in I_1, e.g. for $PI^{0.1}$ controller at the level of ~0.5 %; it cannot be, however, guaranteed – in 4 cases, higher values of I_1 can be noted in comparison with Test I,

- Results of Test III (Figs. 7d-f) suggest the correct convergence of the algorithm to the optimal point in a few main iterations,

- Since the cost function (I_1) is relatively flat, the slight improvement in tracking performance can be observed (see Fig. 8), with the transient behaviour of the closed-loop system presenting the tendency to oscillatory behaviour.

In order to improve the tracking performance, it is expected in further tests to include different cost functions, taking e.g. control effort into account. In further works, a modification to three-parameter off-line iterative framework is planned.

Table 2. Results of tests I and II.

PI^{λ}	K_P		K_I		I_1 (IAE) [10^{-1}]		I_2 (ISE[a]) [10^{-1}]	
λ	Test I	Test II	Test I	Test II	Test I	Test II	Test I	Test II
1.0	24.4814	24.6941	23.8431	28.3910	3.048	3.023	3.337	3.335
0.9	24.7071	24.9858	23.9064	25.6415	3.046	3.022	3.359	3.333
0.8	24.8571	24.9660	18.8231	22.2136	3.040	3.035	3.318	3.332
0.7	23.7901	23.9223	18.4499	19.0481	3.074	3.074	3.333	3.341
0.6	24.4100	29.2277	12.9339	16.2534	3.025	3.027	3.325	3.342
0.5	33.0518	34.3586	9.0905	13.6396	2.997	2.991	3.296	3.307
0.4	38.3518	37.7536	3.6960	6.5126	2.963	2.984	3.266	3.306
0.3	48.4502	48.1355	2.2702	5.1740	2.905	2.917	3.262	3.280
0.2	72.0117	67.9995	10.0191	5.4634	2.832	2.829	3.229	3.227
0.1	90.9809	91.7018	2.5182	7.0100	**2.817**	**2.802**	3.294	3.247

[a] ISE – Integral of Squared Error

REFERENCES

Aleksandrov, D., Penkov, I.: Optimization Mini Unmanned Helicopter Energy Consumption by Changing Geometrical Parameters of Coaxial Rotor Pairs. *Topical Problems in the Field of Electrical and Power Engineering*, pp. 139-141 (2012).

Bellman, R., Cooke, K.L.: Differential-Difference Equations, *Academic Press*, vol. 45, no. 6 (1963) DOI: 10.1002/zamm.19650450612.

Bondyra, A., Gardecki, S., Gąsior, P., Giernacki, W.: Performance of Coaxial Propulsion in Design of Multi-rotor UAVs. Advances in Intelligent Systems and Computing, *Springer*, pp. 523-531 (2016), DOI: 10.1007/978-3-319-29357-8_46.

Bouabdallah, S., Noth, S. and Siegwart, R.: PID vs LQ Control Techniques Applied to an Indoor Micro Quadrotor. In: *Proceedings of the 2004 IEEE/RSJ International Conference on Intelligent Robots and Systems,* pp. 2451-2456 (2004).

Caponetto, R., Dongola, G., Fortuna, L., Petras, I.: Fractional Order Systems Modeling and Control Applications, *World Scientific Series on Nonlinear Science: Singapore*, Series A, no. 72 (2010).

Castillo, P., Lozano, R., Dzul, A.E.: Modeling and Control of Mini-Flying Machines, London: *Springer-Verlag* (2005).

Chen, YQ., Petras, I., Xue, D.: Fractional Order Control A Tutorial, In: *Proc. of the American Control Conference,* pp. 1397-1411, St. Louis, USA (2009).

Chong, E.K.P., Zak, S.H.: An Introduction to Optimization, 2nd ed., New Jersey, *John Wiley & Sons* (2001).

Duan, H., Li, P.: Bio-inspired Computation in Unmanned Aerial Vehicles. Berlin: *Springer-Verlag* (2014).

Durand, S., Boisseau, B., Marchand, N., Guerrero-Castellanos, J.F.: Event-based PID Control: Application to a Mini Quadrotor Helicopter. *Control Engineering and Applied Informatics* 20(1): 36-47 (2018).

Efe, M. Ö.: Fractional Order Systems in Industrial Automation – A Survey. *IEEE Transactions on Industrial Informatics*, 7(4): 582-591 (2011).

Espinoza, T., Dzul, A., Llama, M.: Linear and nonlinear controllers applied to fixed-wing UAV. International *Journal of Advanced Robotic Systems*, 10(33), pp. 1-10 (2013).

Espinoza, T., Dzul, A., Cortes-Martinez F.: Real Time Implementation and Flight Tests using Linear and Nonlinear Controllers for a Fixed-wing Miniature Aerial Vehicle (MAV). *International Journal of Control, Automation and Systems* 16(1): 392-396 (2018).

Fister, D., Fister Jr., I., Fister, J., Safaric, R.: Parameter tuning of PID controller with reactive nature-inspired algorithms. *Robotics and Autonomous Systems* 84: 64-75 (2016).

Gardecki, S., Giernacki, W., Gośliński, J.: Velocity control of drive unit in four-rotor flying robot. In: Proc. of the 10th *International Conference on Informatics in Control, Automation and Robotics* (ICINCO 2013), pp. 245–250 (2013) DOI: 10.5220/0004477002450250.

Gautam, D., Ha, Ch.: Control of a Quadrotor Using a Smart Self-Tuning Fuzzy PID Controller. *International Journal of Advanced Robotics Systems*, 10(380), pp. 1-9 (2013).

Gąsior, P., Bondyra. A., Gardecki, S., Giernacki, W., Kasiński, A.: Thrust estimation by fuzzy modeling of coaxial propulsion unit for multirotor UAVs. In: *IEEE International Conference in Multisensor Fusion and*

Integration for Intelligent Systems (MFI), Baden-Baden, Germany, pp. 418-423 (2016) DOI: 0.1109/MFI.2016.7849524.

Giernacki, W.: Near to Optimal Design of $PI^{\lambda}D^{\mu}$ Fractional-order Velocity Controller (FOPID) For Multirotor Motor-Rotor Simplified Model, In *Proc. of the 2016 International Conference on Unmanned Aircraft Systems* (ICUAS), pp. 320-326, Arlington, USA, (2016a) DOI: 10.1109/ICUAS.2016.7502516.

Giernacki, W., Sadalla, T., Gośliński, J., Kozierski, P., Coelho, J.P., Sladić, S.: Rotational Speed Control of Multirotor UAV's Propulsion Unit based on Fractional-order PI Controller. In: *Proc. 22nd International Conference on Methods and Models in Automation and Robotics*, pp. 993-998, Międzyzdroje, Poland (2017a) DOI: 10.1109/MMAR.2017.8046965.

Giernacki, W., Sadalla T.: Comparison of tracking performance and robustness of the simplified model of multirotor aerial robot with CDM and PID (with anti-windup compensation) controllers. *Journal of Control Engineering and Applied Informatics,* 19(3), pp. 31-40 (2017b).

Giernacki, W., Horla, D., Báča, T., Saska, M.: Real-time model-free optimal auto tuning method for unmanned aerial vehicle controllers based on Fibonacci-search algorithm (2018a, in review).

Giernacki, W., Horla, D., Espinoza-Fraire, T.: Strategy for optimal autotuning of the fixed-wing UAV controllers by the use of zero-order optimization algorithm (2018b, in review).

Giernacki. W., Horla, D., Sadalla, T., Coelho, J.P.: Robust CDM and Pole Placement PID Based Thrust Controllers for Multirotor Motor-Rotor Simplified Model, In: 2016 *International Siberian Conference on Control and Communications* (SIBCON), pp. 1-5, Moscow, Russia (2016b) DOI: 10.1109/SIBCON.2016.7491826.

Guo, R., Dong, J., Zhu, Y.: Disturbance Rejection and Asymptotically Stabilizing Control for a Quadrotor UAV. *Journal of Control Engineering and Applied Informatics,* 17(4), pp. 33-41 (2015).

Hafasi, S., Laabidi, K., Farkh, R.: Synthesis of a fractional PI controller for a first-order time delay system. *Transactions of the Institute of Measurement and Control*, vol. 35, no. 8, pp. 997–1007 (2013).

Killingsworth, N.J., Krstic, M.: PID Tuning Using Extremum Seeking. Model-free for online performance optimization. *IEEE Control Systems*, 26(1): 70-79, (2006).

Magsino, E.R., Dolossa, C.M., Gavinio, S., Hermoso, G., Laco N., Roberto, L.A.: Implementation of Velocity and Torque Control on Quadrotor Altitude and Attitude Stability. *The Manila Journal of Science*, 8(2), pp. 9-20 (2013).

Mahony, R., Kumar, V., Corke, P.: Multirotor Aerial Vehicles: Modeling, Estimation, and Control of Quadrotor. *IEEE Robotics & Automation Magazine*. 19(3): 20-32 (2012).

Pounds, P., Bersak, D.R., Dollar, A.M.: Stability of small-scale UAV helicopters and quadrotors with added payload mass under PID control. *Autonomous Robots* 33(1): 129-142 (2012).

Precup, R-E., Angelov, P., Jales Costa, B.S., Sayed-Mouchaweh, M.: An overview on fault diagnosis and nature-inspired optimal control of industrial process applications. *Computers in Industry*, 74: 75-94 (2015).

Raptis, I.A., Valavanis, K.P.: Linear and Nonlinear Control of Small-Scale Unmanned Helicopters, *Springer* (2011).

Ren, B., Ge, S.S., Chen, C., Fua, C.-H., Lee, T.H.: Modeling, Control and Coordination of Helicopter Systems, *Springer* (2012).

Sanchez, A., Garcia Carrillo, L.R., Rondon, E., Lozano, R., Garcia, O.: Hovering Flight Improvement of a Quad-rotor Mini UAV Using Brushless DC Motors. *Journal of Intelligent Robotic Systems,* vol. 61, pp. 85-101 (2011).

Saska, M., Vonasek, V., Chudoba, J., Thomas, J., Loianno, G., Kumar, V.: Swarm Distribution and Deployment for Cooperative Surveillance by Micro-Aerial Vehicles. *Journal of Intelligent and Robotic Systems*, 84: 469-492 (2016).

Szafrański, G., Czyba, R., Błachuta, M.: Modeling and identification of electric propulsion system for multirotor unmanned aerial vehicle design. In: *Proc. of the 2014 International Conference on Unmanned Aircraft Systems*, pp. 470–476 (2014).

Tepljakov, A.: Fractional-order Modeling and Control of Dynamic Systems, *Springer* (2017).

Tepljakov, A., Petlenkov, E., Belikov, J., Finajev, J.: Fractional-order controller design and digital implementation using FOMCON toolbox for MATLAB. In: *Proc. of the IEEE Conference on Computer Aided Control System Design* (CACSD), pp. 340–345 (2013)

Valavanis, K., Vachtsevanos, G.J.: Handbook of Unmanned Aerial Vehicles, *Springer* (2015).

Won Kim, H., Brown, R.E.: A Comparison of Coaxial and Conventional Rotor Performance. *Journal of the American Helicopter Society*, 55(1), pp.1-20 (2010).

Zelazo, D., Franchi, A., Bulthoff, H.H., Giordano P.R.: Decentralized rigidity maintenance control with range measurements for multi-robot systems. *International Journal of Robotics Research*, 34(1), pp. 105-128 (2015).

Appendix A. Hermite-Biehler Theorem

(Caponetto et al., 2010; Hafasi et al., 2013)

Let δ be a complex function of ω described by equation (8), where $\delta_r^*(\omega)$ and $\delta_i^*(\omega)$ represent the real and imaginary parts of $\delta^*(j\omega)$. The $\delta^*(j\omega)$ is stable if:

$\delta_r^*(\omega)$ and $\delta_i^*(\omega)$ only have simple real roots and these are interlaced;

$\delta_i^{'*}(\omega)\delta_r^*(\omega) - \delta_i^*(\omega)\delta_r^{'*}(\omega) > 0$, for some *some* $\omega=\bar{\omega}$ in $(-\infty,+\infty)$,

where $\delta_i^{'*}(\omega)$ and $\delta_r^{'*}(\omega)$ are the derivatives of $\delta_i^*(\omega)$ and $\delta_r^*(\omega)$ with respect to ω. An important step is to ensure that

$\delta_i^*(\omega)$ and $\delta_r^*(\omega)$ only have real roots. This can be achieved by applying the Pontryagin Theorem.

Appendix B. Pontryagin Theorem

Let $\delta^*(s)$ be described by the equation (7) assuming $s=j\omega$.

To assure that $\delta_i^*(\omega)=0$ and $\delta_r^*(\omega)=0$ only have real roots, it must be assured that in interbals

$$-2l\pi+\eta \le \omega \le 2l\pi+\eta \quad l=1,2,3,..., \tag{B1}$$

$\delta_i^*(\omega)$ and $\delta_r^*(\omega)$ have exactly $4lN+M$ roots. For situation where characteristic equation is of fractional order, the $\delta_i^*(\omega)$ and $\delta_r^*(\omega)$ must have $4l([N]+1)+[M]+1$ roots, where [...] represents the integer part, and N and M are taken as degree of the numerator and denominator polynomials of the integer part.

Proofs can be found in (Caponetto et al., 2010).

Appendix C. $\delta_r^*(\omega)$ and $\delta_i^*(\omega)$ calculation for the FOPI controller

Rewriting the $\delta(s)=0$ quasi-polynomial from equation (7) for transfer function $C(s)$ of controller from equation (6), following equation can be written:

$$\delta^*(s)=b_0K_Ps^{\lambda}+b_0K_I+(a_1s+a_0)e^{sL}s^{\lambda}. \tag{C1}$$

For $g=Ls$ and $\lambda=a/b$ equation (C1) takes the form:

$$\delta^*(g)=b_0K_P(g/L)^{a/b}+b_0K_I+(a_1g/L+a_0)e^{g}(g/L)^{a/b}, \tag{C2}$$

and for $g=j\omega$ it is true that

$$\begin{aligned}\delta^*(j\omega)&=b_0K_P(j\omega/L)^{a/b}+b_0K_I\\&+(a_1j\omega/L+a_0)e^{j\omega}(j\omega/L)^{a/b}.\end{aligned} \tag{C3}$$

Finally, after replacing the $e^{j\omega}$ with $\cos(\omega)+j\sin(\omega)$, the real $\delta_r^*(\omega)$ and imaginary $\delta_i^*(\omega)$ parts of $\delta*(\omega)$ can be described by following two equations:

$$\begin{aligned}\delta_r^*(\omega)&=\left[b_0K_P+a_0\cos(\omega)-\frac{a_1\omega\sin(\omega)}{L}\right]\cdot\\&\cdot\left|\mathrm{Re}(j)^{a/b}\right|\frac{|\omega^{a/b}|}{L^{a/b}}+b_0K_I-\left[\frac{a_1\omega}{L}\cos(\omega)+a_0\sin(\omega)\right],\\&\cdot\left|\mathrm{Im}(j)^{a/b}\right|\frac{|\omega^{a/b}|}{L^{a/b}}sign(\omega),\end{aligned} \tag{C4}$$

$$\begin{aligned}\delta_i^*(\omega)&=\left[b_0K_P+a_0\cos(\omega)-\frac{a_1\omega\sin(\omega)}{L}\right]\cdot\\&\cdot\left|\mathrm{Im}(j)^{a/b}\right|\frac{|\omega^{a/b}|}{L^{a/b}}sign(\omega)-\left[\frac{a_1\omega}{L}\cos(\omega)+a_0\sin(\omega)\right]\cdot\\&\cdot\left|\mathrm{Re}(j)^{a/b}\right|\frac{|\omega^{a/b}|}{L^{a/b}}.\end{aligned} \tag{C5}$$